5-1-2014

Stellar Parameters of Three Massive Stars in Cygnus OB2

Kathryn V. Lester
Lehigh University

M. Virginia McSwain
Lehigh University

Recommended Citation

Lester, Kathryn V. and McSwain, M. Virginia, "Stellar Parameters of Three Massive Stars in Cygnus OB2" (2014). *Eckardt Scholars Projects*. 17.
https://preserve.lehigh.edu/undergrad-scholarship-eckardt/17

Eckardt Scholars Senior Thesis, 2014

Stellar Parameters of Three Massive Stars in Cygnus OB2

Kathryn V. Lester[1], M. Virginia McSwain[1] and Henry A. Kobulnicky[2]

ABSTRACT

We report stellar parameters for three massive stars in the Cygnus OB2 Association: MT216, MT234, and MT485. By comparing spectra from the Cygnus OB2 Radial Velocity Survey to Tlusty model spectra, we determined the best fit effective temperature (T_{eff}), surface gravity ($\log g$), and observed rotational velocity ($v \sin i$). We calculated the χ^2 error for each model, and then used the best fit parameters to determine the spectroscopic mass of each star.

---

[1] Dept. of Physics, Lehigh University, Bethlehem, PA, 18015

[2] Dept. of Physics & Astronomy, University of Wyoming, Laramie, WY, 82070

1. Introduction

Massive stars have more than ten times as much mass as the Sun, and are also the hottest and brightest types of stars, known as O and B type stars. These stars evolve by expanding to become red supergiant stars, and then end their lives by exploding as core-collapse supernovae. This explosion disperses all of the star's material into interstellar space and forms rich gas clouds, which then form new generations of stars and planets. The Cygnus OB2 Association is the home to thousands of these O and B type stars, about 5000 lightyears away our galaxy. In hopes of aiding statistical studies of the stellar evolution of massive stars, we report stellar parameters for three massive stars in the Cygnus OB2 Association: MT216, MT234, and MT485[1].

2. Observations

We used observations from the WIRO[2] and WIYN[3] telescopes taken as part of the Cygnus OB2 Radial Velocity Survey. Our WIRO data were taken during the summer of 2013 with wavelength $5400 - 6800$Å (Kobulnicky et al. 2014), and our WIYN data were taken from 2001-2008 with wavelength $3800 - 4500$Å (Kiminki et al. 2007). A list of observation dates for each star is shown in Tables 1, 2, and 3. The spectra were reduced using standard techniques in IRAF, including flat fielding, wavelength calibration between each exposure, and heliocentric Doppler corrections. These reductions ignore light from the sky, remove instrumental errors, and correct for the fact that the Earth is not stationary. For the wavelength calibration, WIRO uses copper-argon lamps, while WIYN uses helium-neon-argon lamps to assign wavelengths to each absorption line. In order to further reduce the noise in our spectra, we matched the wavelength scale of each spectrum and averaged them together for each star to use in comparison with the models.

3. Data Analysis

Since the effective temperature and surface gravity of a star changes the shape of its absorption lines, a spectra model that best reproduces the shape of the absorption lines would thus correspond to the parameters of the star. Using this method, we wrote an IDL program to fit Tlusty model spectra (Lanz & Hubeny 2003, 2007) to our spectra in order to determine their effective temperature (T_{eff}), surface gravity ($\log g$), and observed rotational velocity ($v \sin i$). We used the solar abundance OSTAR2002 models for MT485 (spectral type O8). The O-star T_{eff} range is $27500 - 55000$K with 2500K spacing, and the $\log g$ range is $3.0 - 4.75$ with 0.25 spacing. We used solar abundance

---

[1] Using the nomenclature of Massey & Thompson. (1991)

[2] Wyoming Infrared Observatory, Mt. Jelm, WY

[3] Wisconsin-Indiana-NOAO Telescope, Kitt Peak, AZ

BSTAR2006 models for MT216 (spectral type B1) and MT234 (spectral type B2). The B-star T_{eff} range is $15000 - 30000$K with 1000K spacing, and the $\log g$ range is $3.0 - 4.75$ with 0.25 spacing.

We read in the Tlusty models for each combination of T_{eff} and $\log g$ for comparison against the star's observed spectra. We first shifted the star's observed spectrum by dividing by the slope of the continuum line, so that the observed continuum was aligned with the continuum of the models. We then corrected for two types of broadening for the model spectra: rotational and instrumental broadening. A star's rotation causes the emitted light on the edges of a star to be Doppler shifted, so the absorption lines become slightly wider. We calculated the best fit $v \sin i$ for each star to use when correcting for rotational broadening using the λ4471Å helium line, since the strength of helium absorption lines are dependent primarily on the star's rotational speed. Instrumental broadening results from limitations of the telescope's optics, which do not allow for infinitely precise measurements. For instrumental broadening, we convolved the model spectra with a Gaussian of FWHM of 2.0Å.

We used hydrogen absorption lines to calculate the χ^2, since hydrogen lines vary with the temperature and surface gravity of the star. We first applied the models to the WIRO spectra, but the λ6563Å $H\alpha$ line did not vary enough to find a best fit model. We then used the WIYN spectra, with which we had more success using the λ4340Å $H\gamma$ line. We calculated the χ^2 value for each of the temperature and gravity pairs using the equation

$$\chi^2 = \Sigma(O - C)^2 \tag{1}$$

We then calculated the 1σ, 2σ, and 3σ error ranges using equation 2 and found which pairs of stellar parameters fell within each error range.

$$\chi^2_{acceptable} = \chi^2_{min} + range_\sigma \tag{2}$$

where the 1σ, 2σ, and 3σ error ranges are

$$range_{1\sigma} = \chi^2_{min} * 2.30 \tag{3}$$

$$range_{2\sigma} = \chi^2_{min} * 4.61 \tag{4}$$

$$range_{3\sigma} = \chi^2_{min} * 9.21 \tag{5}$$

.

4. Results

The best fit parameters for each star are summarized in Table 4. Plots showing the observed and model spectra around the $H\gamma$ line are shown in Figures 1, 2, and 3, and the χ^2 contour plots for each star are shown in Figures 4, 5, and 6.

We then compared best fit parameters to the evolutionary models of Schaller et al. (1992) to determine the mass, age and radius estimates for each star, shown in Table 5. These parameters are only estimates, however, since the error bars are quite large. The masses found by Kobulnicky et al. (2014) using orbital motion are also shown in Table 5.

4.1. MT216

Since the observed spectra for this star are very noisy, we were not able to average several spectra together in order to reduce the noise. Only one night's data were used for this analysis, and therefore, the error bars for the best fit parameters for MT216 are quite large. Also, the spectra for MT216 has an abnormal peak in the right wing of the hydrogen-γ line from a cosmic ray, so we did not include those points in the fit.

Kobulnicky et al. (2014) did not find MT216 to be a binary star since its radial velocity variations were quite irregular. We were able to determine the best fit parameters to be $T_{eff} = 27,000$K, $\log g = 4.00$, and $v \sin i$ =35 kms^{-1}, and then estimated the spectroscopic mass to be $12.6 M_{sun}$. The fit around the $H\gamma$ line is shown in Figure 1, and the χ^2 contour plot for MT216 is shown in Figure 4.

4.2. MT234

MT234 is a long period spectroscopic binary, with a period of 13.96 years (Kobulnicky et al. 2014). We found the primary star to have best fit parameters of $T_{eff} = 23,000$K, $\log g = 4.00$, and $v \sin i$ =55 kms^{-1}, and then estimated the spectroscopic mass to be $9.2 M_{sun}$. The fit around the $H\gamma$ line is shown in Figure 2, and the χ^2 contour plot for MT234 is shown in Figure 5. This star's spectra had the best signal to noise ratio since we were able to average several good-quality spectra together, and therefore this star has the smallest error range for its best fit parameters.

4.3. MT485

MT485 is a long period spectroscopic binary, with a period of 11.13 years (Kobulnicky et al. 2014). We found the primary star to have best fit parameters of $T_{eff} = 47,500$K, $\log g = 4.50$, and $v \sin i$ =80 kms^{-1}, and then estimated the spectroscopic mass to be $36.1 M_{sun}$. The fit around the $H\gamma$ line is shown in Figure 3, and the χ^2 contour plot for MT485 is shown in Figure 6.

For hot O type stars, the $H\gamma$ line (for neutral hydrogen) does not vary much with temperature, since most of the star's hydrogen is already ionized. So our error bars for the best fit parameters of MT485 are quite large. Another method of determining temperature would be to use the ratio of strengths of the singly ionized helium (He II) lines to the neutral helium (He I) lines, so further analysis could be done to narrow the range of acceptable stellar parameters.

5. Discussion

The spectroscopic mass matched the mass found from orbital motion for MT216 but not MT485. This is a common problem for O-stars, called ”the Mass Discrepancy” (Massey et al. 2012). This indicated that the models are somehow flawed, misrepresenting some property of massive stars such as their intense stellar wind. Astronomers are still working to understand this discrepancy.

Nonetheless, all three of these stars will eventually explode as core-collapse supernovae based on their mass estimates. Models of the evolutionary tracks of massive stars are shown in Figure 7. The graph shows that the stars will expand, thus becoming redder and brighter, as they evolve (Schaller et al. 1992). Massive stars burn hydrogen, helium, and all of the elements until nickel. Burning nickel no longer produces energy during fusion, so the stars stop emitting light. Their immense force of gravity is no longer balanced by radiation pressure, and the stars collapse and explode as supernovae. MT216 and MT234 will likely collapse to form a neutron star, where the star becomes so dense that the electrons are packed into the nucleus. MT485 would most likely condense further to form a black hole, where all of the mass condenses to a single point.

In conclusion, the mass estimates for these stars determine how they will evolve, as described above. The best fit parameters found in this work will hopefully aid statistical studies of the Cygnus OB2 Association, so astronomers can further understand the formation and evolution of massive stars.

ACKNOWLEDGEMENTS

Katie Lester is grateful to Dr. Ginny McSwain for all of her help and guidance, Dr. Chip Kobulnicky for giving us the data, and the Eckardt Scholars program.

REFERENCES

Kiminki, D. C., Kobulnicky, H. A., Kinemuchi, K., et al. 2007, ApJ, 664, 1102

Kobulnicky, H. A., et al. 2014, ApJ, in press

Lanz, T., & Hubeny, I. 2003, ApJS, 147, 225

Lanz, T., & Hubeny, I. 2007, ApJS, 169, 83

Martins, F., Schaerer, D., & Hillier, D. J. 2002, A&A, 382, 999

Massey, P., & Thompson, A. B. 1991, ApJ101, 1408

Massey, P., Morrell, N. I., Neugent, K. F., et al. 2012, ApJ, 748, 96

Schaller, G., Schaerer, D., Meynet, G., & Maeder, A. 1992, A&AS, 96, 296

This preprint was prepared with the AAS LaTeX macros v5.2.

Table 1: List of observation dates.

Star	Telescope	Date
MT216	WIYN	2001 September 8
	WIRO	2012 October 10
	WIRO	2012 October 14
	WIRO	2013 June 17
	WIRO	2013 June 20
	WIRO	2013 July 1
	WIRO	2013 July 15
	WIRO	2013 July 16
	WIRO	2013 July 23
	WIRO	2013 July 26
	WIRO	2013 August 15
	WIRO	2013 October 8

Table 2: List of observation dates.

Star	Telescope	Date
MT234	WIYN	2001 August 24
	WIYN	2001 September 8
	WIYN	2001 September 9
	WIYN	2004 November 30
	WIYN	2006 September 10
	WIRO	2011 May 31
	WIRO	2011 June 4
	WIRO	2011 June 24
	WIRO	2011 June 28
	WIRO	2011 July 23
	WIRO	2011 August 7
	WIRO	2011 August 8
	WIRO	2011 August 21
	WIRO	2012 July 9
	WIRO	2012 August 26
	WIRO	2012 September 7
	WIRO	2013 June 16
	WIRO	2013 June 20
	WIRO	2013 June 24

Table 3: List of observation dates.

Star	Telescope	Date
MT485	WIYN	2006 September 10
	WIYN	2001 August 24
	WIYN	2001 September 8
	WIYN	2001 September 9
	WIYN	2004 November 29
	WIYN	2008 June 12
	WIRO	2011 June 1
	WIRO	2011 June 2
	WIRO	2011 June 5
	WIRO	2011 June 24
	WIRO	2011 June 26
	WIRO	2011 June 27
	WIRO	2011 July 14
	WIRO	2011 July 25
	WIRO	2011 August 7
	WIRO	2011 August 20
	WIRO	2011 August 31
	WIRO	2011 September 29
	WIRO	2011 October 31
	WIRO	2012 May 28
	WIRO	2012 June 1
	WIRO	2012 June 13
	WIRO	2012 June 18
	WIRO	2013 June 16
	WIRO	2013 June 24
	WIRO	2013 June 27

Table 4: Best fit stellar parameters from our spectral fitting.

Star	Spectral Type	T_{eff} (K)	$\log g$	$v \sin i$ (kms^{-1})
MT216	B1 V	27000^{+3000}_{-12000}	$4.00^{+0.5}_{-1.0}$	35^{+25}_{-18}
MT234	B2 V	23000^{+7000}_{-3000}	$4.00^{+0.5}_{-0.3}$	55^{+12}_{-14}
MT485	O8 V	47500^{+7500}_{-20000}	$4.50^{+0.25}_{-1.25}$	80^{+40}_{-30}

Table 5: Mass, age, and radius estimates from the models of Schaller et al. (1992).

Star	Spectral type	Mass from spectroscopy	Mass from orbital motion	Age of star	Current radius
MT216	B1 V	12.6 M_{sun}	n/a	6.8 x 10^6 yr	5.9 R_{sun}
MT234	B2 V	9.2 M_{sun}	11 M_{sun}	13.3 x 10^6 yr	5.0 R_{sun}
MT485	O8 V	36.1 M_{sun}	21 M_{sun}	$<$ 1.0 x 10^6 yr	5.7 R_{sun}

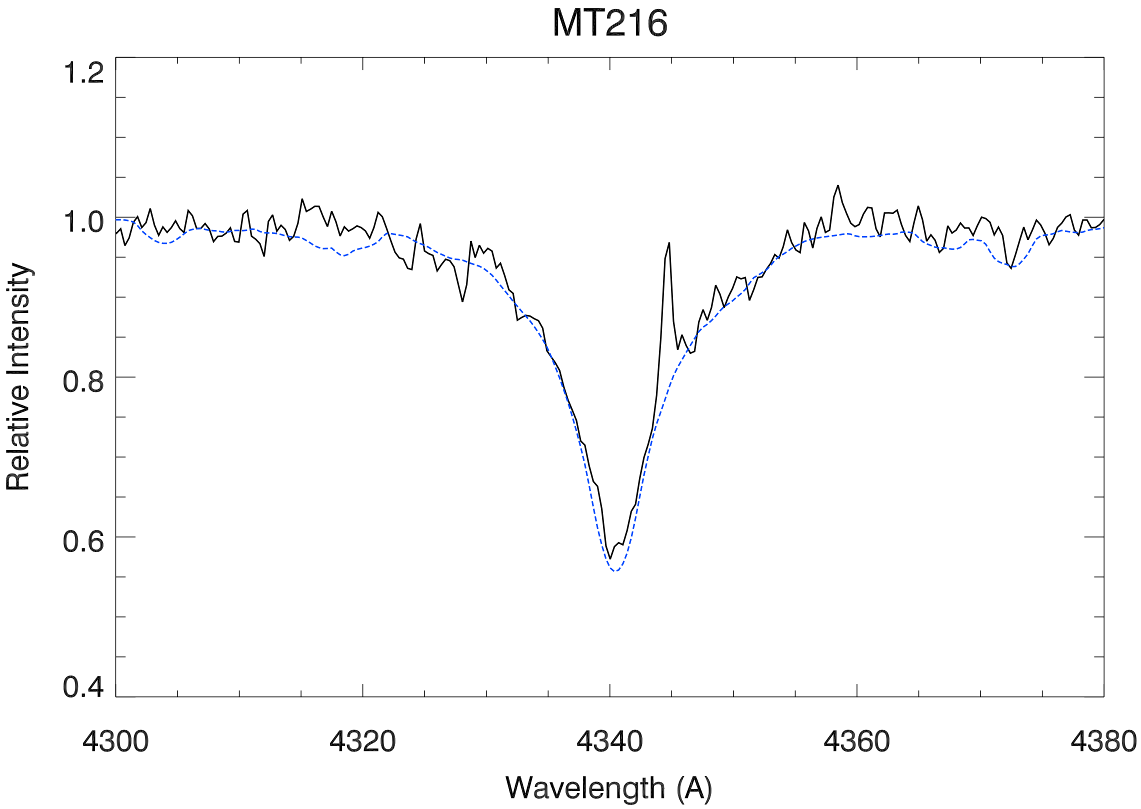

Fig. 1.— The WIYN spectrum of MT216 is shown as the solid line. The best fit model spectrum, with $T_{eff} = 27000$ K, $\log g = 4.00$, and $v \sin i = 35$ kms^{-1} is shown as the blue dashed line.

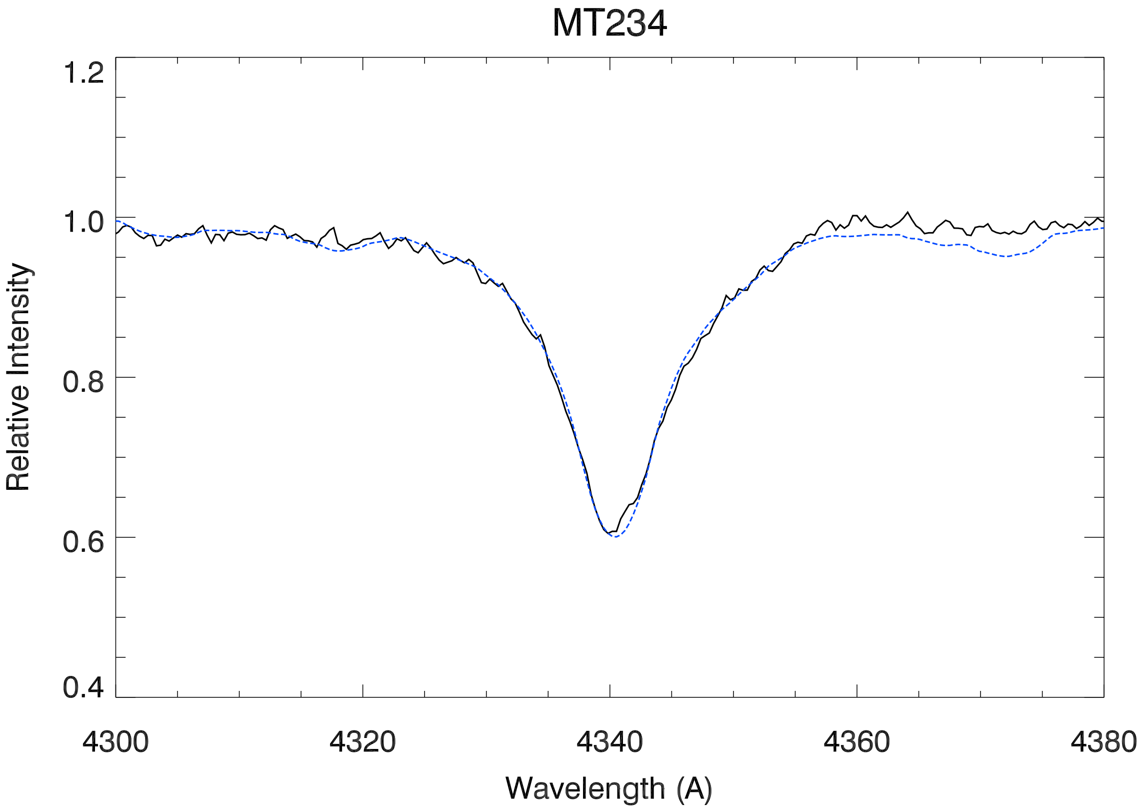

Fig. 2.— The WIYN spectrum of MT234 is shown as the solid line. The best fit model spectrum, with $T_{eff} = 23000$ K, $\log g = 4.00$, and $v \sin i = 55$ kms^{-1} is shown as the blue dashed line.

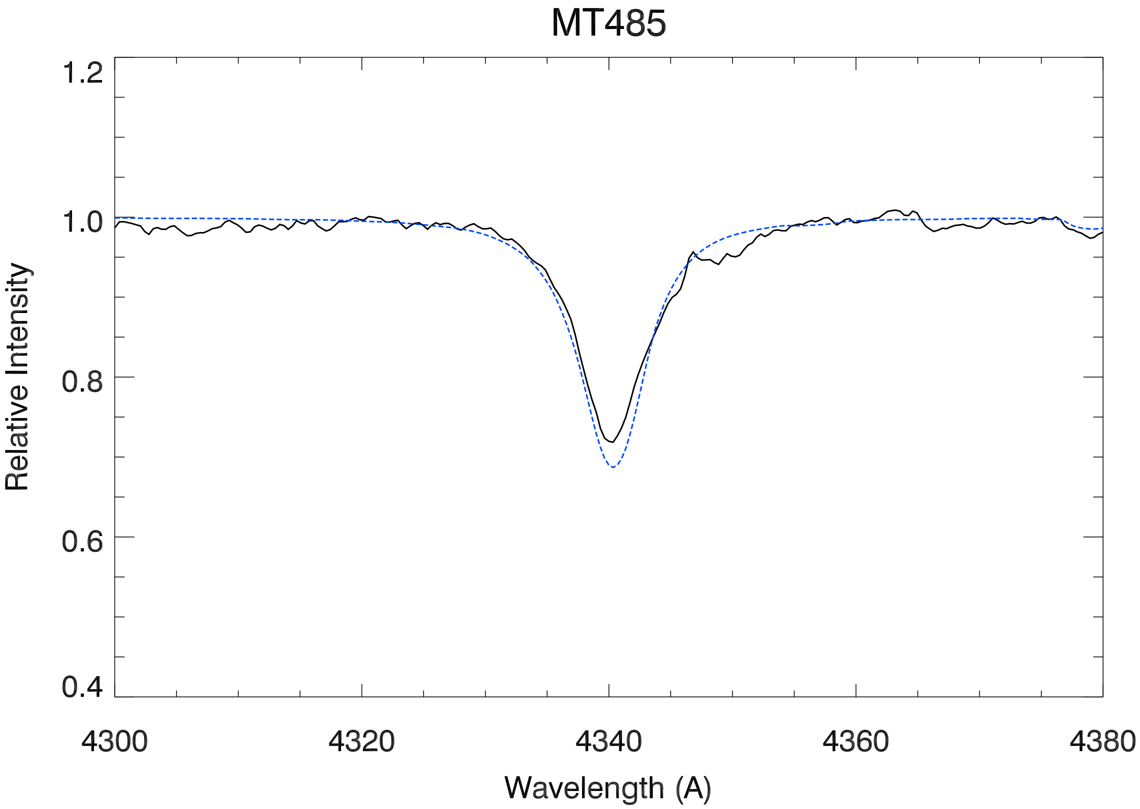

Fig. 3.— The WIYN spectrum of MT485 is shown as the solid line. The best fit model spectrum, with $T_{eff} = 47500$ K, $\log g = 4.50$, and $v \sin i = 80$ kms^{-1} is shown as the blue dashed line.

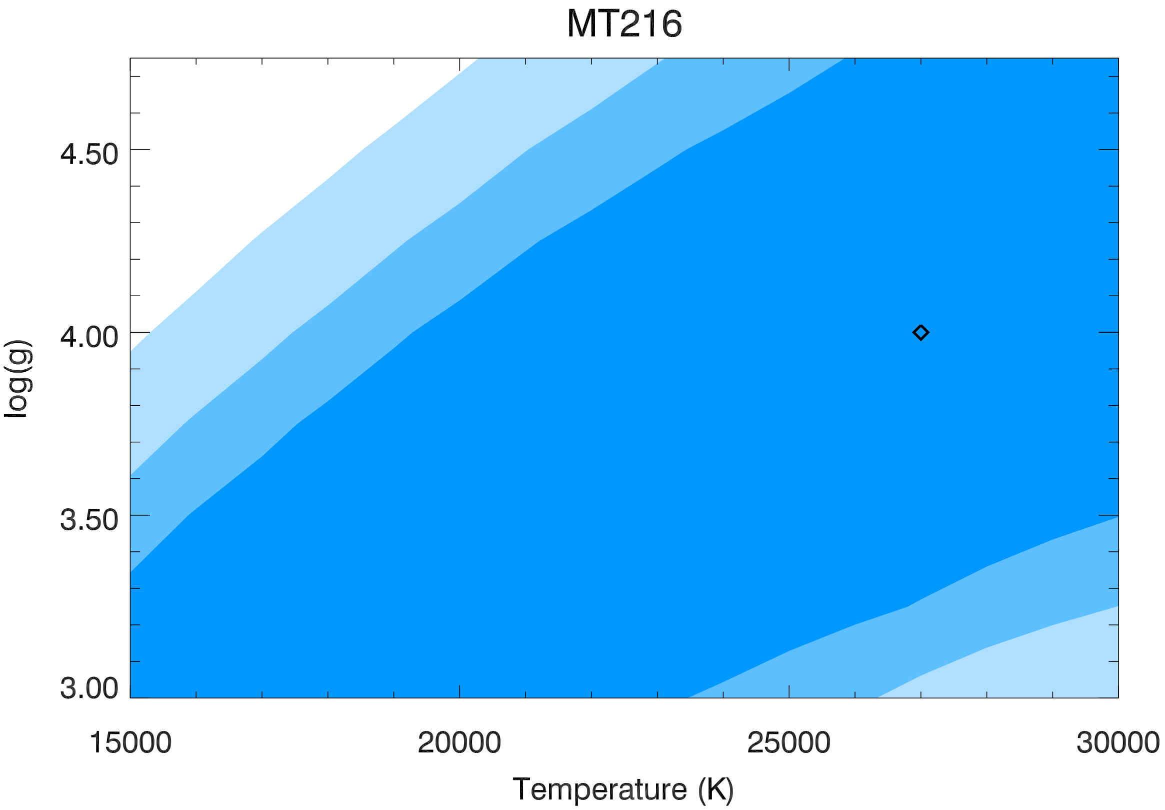

Fig. 4.— A contour plot for the χ^2 error using $v \sin i = 35$ kms^{-1}. The dark, medium, and light blue corresponds to the 1σ, 2σ, and 3σ error ranges, respectively. The diamond marks the model with the lowest χ^2 value.

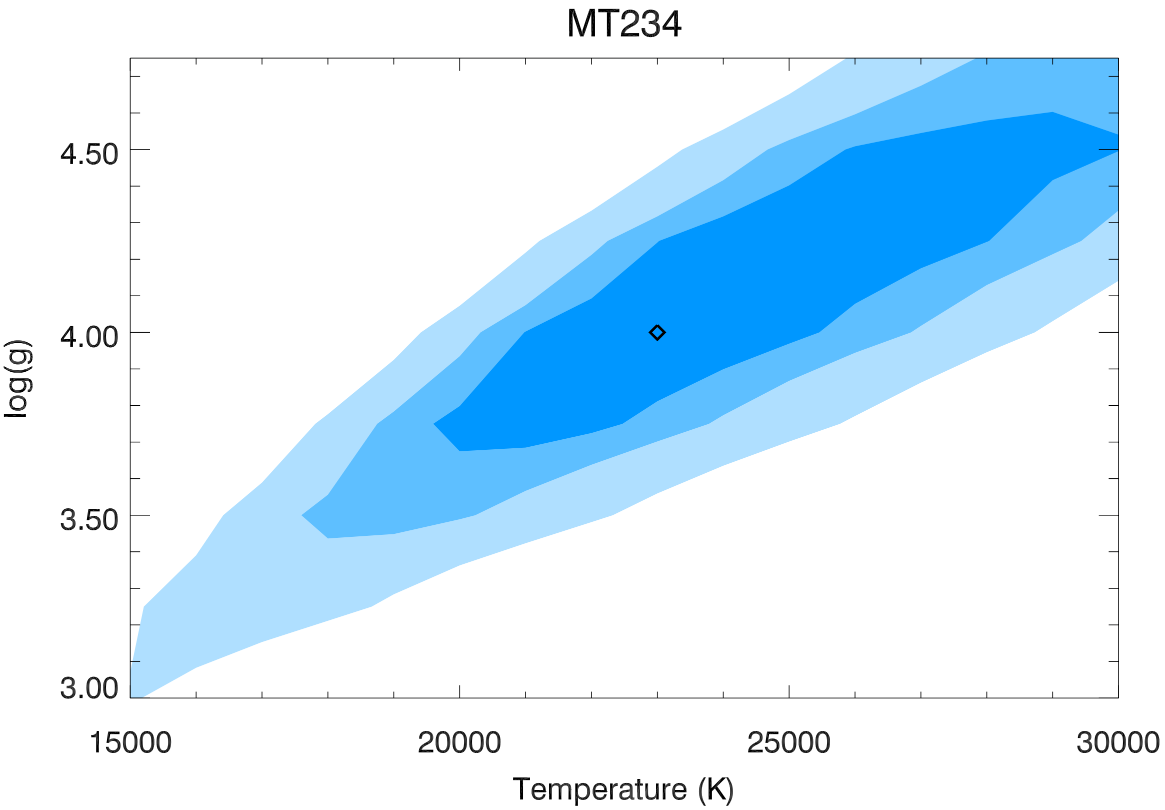

Fig. 5.— A contour plot for the χ^2 error using $v \sin i = 55$ kms^{-1}. The dark, medium, and light blue corresponds to the 1σ, 2σ, and 3σ error ranges, respectively. The diamond marks the model with the lowest χ^2 value.

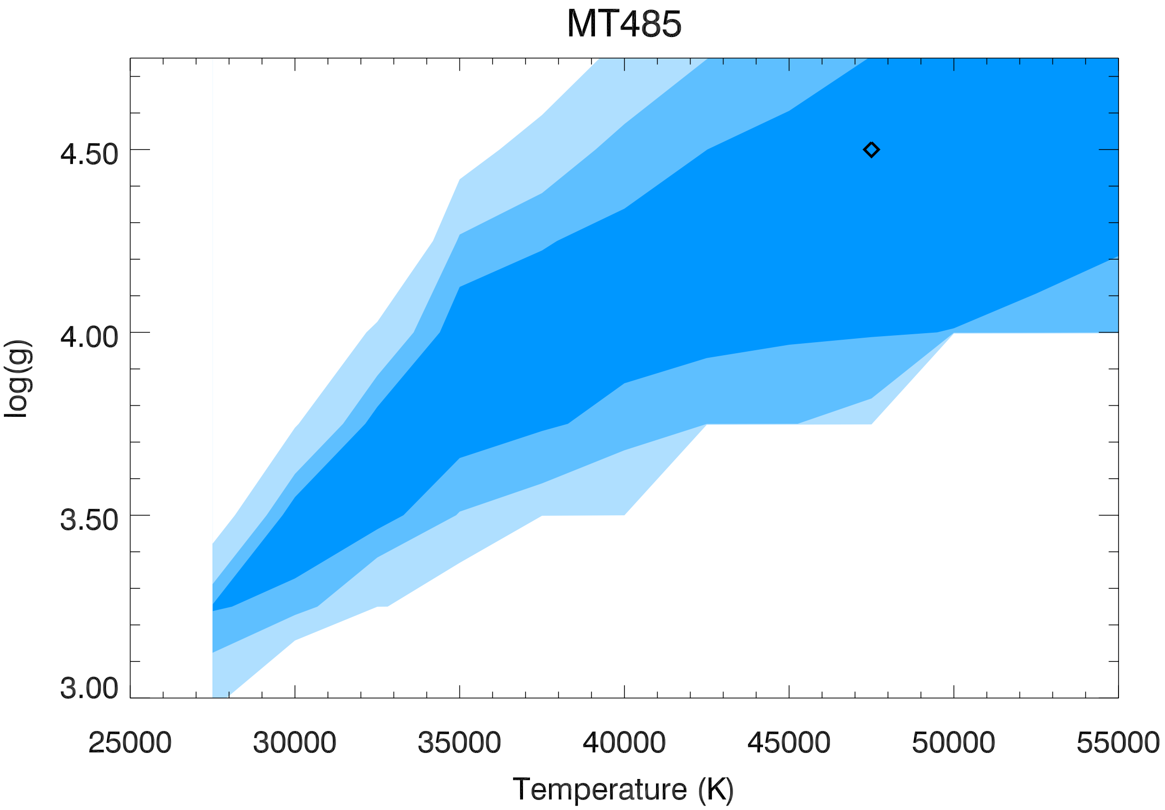

Fig. 6.— A contour plot for the χ^2 error using $v \sin i = 80$ kms^{-1}. The dark, medium, and light blue corresponds to the 1σ, 2σ, and 3σ error ranges, respectively. The diamond marks the model with the lowest χ^2 value.

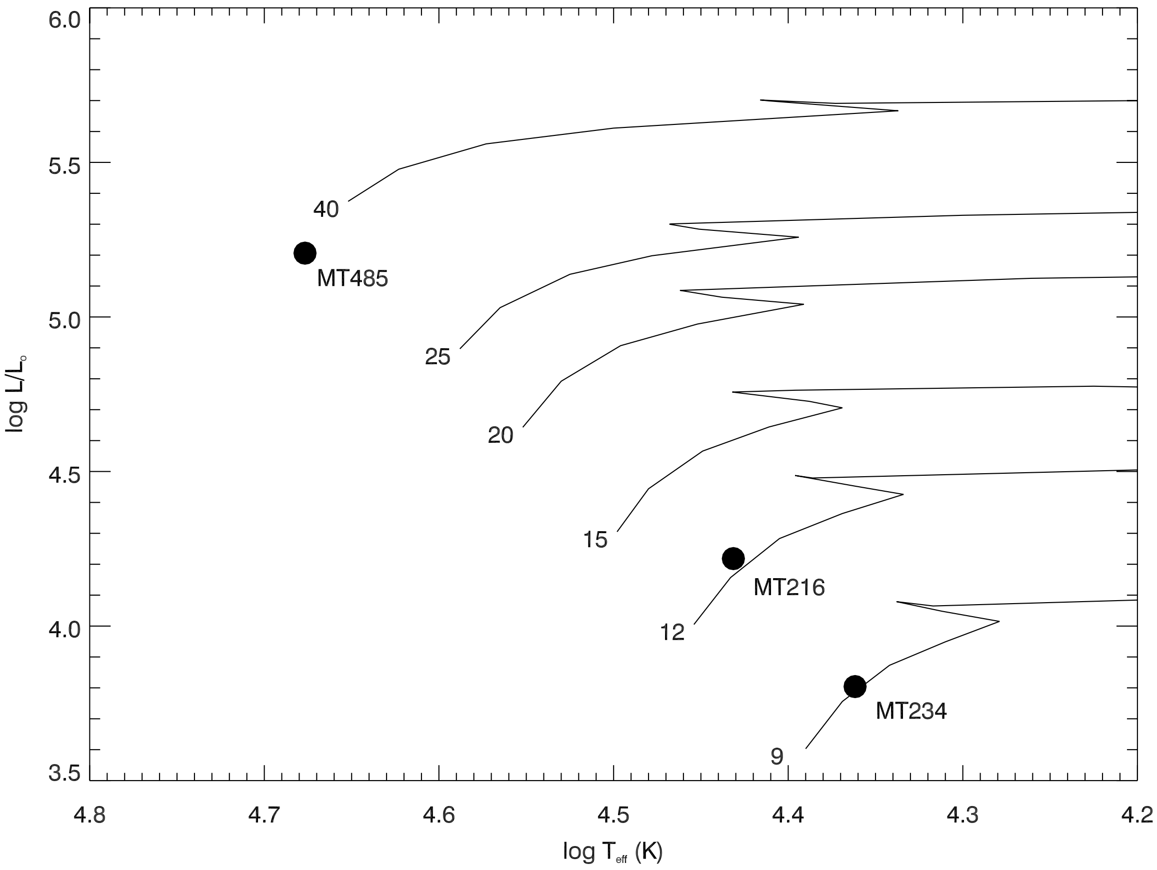

Fig. 7.— The evolutionary tracks for massive stars. MT216, MT234, and MT485 are labeled based on their spectroscopic masses and age estimates. Before the zig zag, the stars are burning hydrogen and are growing slightly cooler (redder) and brighter. The zig zag in the curves corresponds to the stars ending hydrogen burning, where the stars contract slightly. After the zig zag, the stars begin to expand rapidly until helium fusion begins (not shown on the plot). (Schaller et al. 1992)